**IEEE Access**
Multidisciplinary : Rapid Review : Open Access Journal

# Electrostatic Micro-Electro-Mechanical-Systems (MEMS) Devices: a Comparison among Numerical Techniques for Recovering the Membrane Profile

**MARIO VERSACI[1], (Senior Member, IEEE), ALESSANDRA JANNELLI[2], AND GIOVANNI ANGIULLI[3], (Senior Member, IEEE)**

[1]Department of Civil, Energy, Environmental and Materials Engineering, Mediterranea University, I-89122 Reggio Calabria (Italy)
[2]Department of Mathematics and Information Sciences, Physical Sciences, Earth Science, Messina University, Viale Stagno d'Alcontres, I-98166 Messina (Italy)
[3]Department of Information, Infrastructures and Sustainable Energy Engineering, Mediterranea University, I-89122 Reggio Calabria (Italy)

Corresponding author: Giovanni Angiulli (e-mail: giovanni.angiulli@unirc.it).

**ABSTRACT** In this work, numerical techniques based on Shooting procedure, Relaxation scheme and Collocation technique have been used for recovering the profile of the membrane of a $1D$ electrostatic Micro-Electro-Mechanical-Systems (MEMS) device whose analytic model considers $|\mathbf{E}|$ proportional to the membrane curvature. The comparison among these numerical techniques has put in evidence the pros and cons of each numerical procedure. Furthermore, useful convergence conditions which ensure the absence of ghost solutions, and a new condition of existence and uniqueness for the solution of the considered differential MEMS model, are obtained and discussed.

**INDEX TERMS** Electrostatic MEMS Devices, Non-Linear Ordinary Differential Models, Shooting method, Keller-Box Scheme, Lobatto Formulas, Ghost Solutions.

## I. INTRODUCTION

Today there is a growing demand to design high-performance sensors and actuators for cutting-the-edge engineering applications [1]. In such a context, static and dynamic Micro-Electro-Mechanical-Systems (MEMS) technology plays a lead role in implementing these devices [2]. Combining among them micro-size mechanical and electronic devices, MEMS technology, emerged in the second half of the 1960s [3], is now considered as one of the most promising technologies of the 21th century [4],[5]. The industrial usages of MEMS are incredibly varied, ranging from surgical-diagnostic-therapeutic microsystem [6], bio-sensors [7], and tissue engineering [8] to wireless and mobile applications [9]. Furthermore, MEMS are considered extremely interesting for mechatronics applications, because of their small size as well as the easy of realization with relatively low costs [10]. During the years, the advancement in MEMS technology has gone hand in hand with the development of sophisticated the-

oretical models that more and more adhering to the physics underlying the operation of these devices [2], [5]. Recently, some remarkable results have been achieved in several relevant cases, such as thermo-elastic [11], electro-elastic [12], and magnetically actuated systems [13]. However, almost all these models are often structured in an implicit form that does not allow to evaluate explicit analytic solutions [14]. Accordingly, these have to be necessarily computed numerically [15]. However, to validate these computational results, analytical conditions ensuring the existence, uniqueness, and regularity of the solutions have to be derived [16]. To this aim, many mathematical models have been theoretically conceived by using suitable functional spaces [14]. Along this line, Cassani and coauthors presented in [17] a sophisticated non-linear differential mathematical model of a MEMS device, which, due to its intrinsic complexity, has been subsequently simplified neglecting the inertial and non-local effects [18]. Now, starting from this simplified model,

**IEEE** *Access*

Di Barba et al. have been proposed a new elliptical semi-linear dimensionless model of a 1D membrane MEMS, based on the proportionality between the electric field magnitude $|\mathbf{E}|$ and the curvature of the membrane, achieving results of the existence and uniqueness for the solution [19]. In [20] this model was numerically solved by Angiulli et al. by using the Shooting method, whereas in [23] Versaci et al. have developed a new condition of the uniqueness of the solution depending from the material properties and by geometrical characteristics of the device. Based on this premises, in this work we study and compare the numerical performances of Shooting procedure, Relaxation scheme, and Collocation technique in order to reconstruct the MEMS profile membrane. In particular, the Shooting method is an iterative procedure capable of transforming a 1D boundary value problem into an equivalent initial value problem so that the procedure resembles that adopted by a soldier who knows the arrival point of a bullet's trajectory, but who is in a position to be able to control only the initial values: position of the cannon and speed or height of the shot. he is therefore forced to proceed by attempts, observing the subsequent results in terms of distance from the target and correcting the rise [21, 22]. Concerning the Relaxation procedure, it replace an ordinary differential equation by finite-difference equations on mesh guessing a solution on this mesh. Mathematically, finite-difference equations are just algebraic relations between unknowns. The use of iterative technique to relax this solution allow to get the true solution [21, 22]. Finally, the collocation methods impose the satisfaction of the differential equation only in selected points of the definition interval. This is equivalent to placing in the internal nodes the differential equation assigned after approximation of the differential operator with an algebraic equivalent, as well as to satisfy the boundary conditions in the edge nodes. The methods summarly described above are notoriously the most effective and efficient for solving numerically boundary value problems. Furthermore, in the literature, regarding the study of electrostatic membrane MEMS, there are no studies comparing the performances obtained with these procedures [21, 22]. Furthermore, we provide new algebraic conditions able to avoid ghost solutions, i.e. numerical solution which do not fit the condition of existence and uniqueness associated to the analytic differential model at hand [20]. As a final result, a new theoretical condition of existence and uniqueness for the solution, which depends from the electromechanical properties of the membrane, is demonstrated. The paper is organized as follows. Section II provides a description of the 1D electrostatic MEMS device considered in this work. The numerical procedures exploited to recover the membrane profile are detailed in section III. In section IV numerical results, carried out by using the Matlab R2017a environment running on an Intel Core 2 CPU at 1.45GHZ, are presented. In section V the convergence criteria for the considered numerical methods are discussed. Results concerning the existence and the uniqueness of the solution as a function of the electromechanical properties of the membrane are

demonstrated in section VI. In section VII are illustrated the issues regarding the problem of the ghost solutions. Section VIII reports a discussion about the range of parameters for the correct use of the device. Finally, in section IX some conclusive remarks and future perspectives are given.

## II. BASICS ON THE 1D ELECTROSTATIC MEMS DEVICE MODEL

### A. THE ANALYTIC MODEL

The membrane electrostatic MEMS device considered in this study is shown in Fig. 1a. The upper plate is fixed, whereas the lower plate has constrained at its edges a membrane. The membrane deforms towards the top plate when an external voltage $V$ is applied. The corresponding dimensionless model is:

$$\begin{cases} \frac{d^2y(x)}{dx^2} = -\frac{\lambda^2}{(1-y(x))^2}, & x \in \Omega = [-L, L], \\ y(x) = 0, & x \in \partial\Omega \end{cases} \quad (1)$$

where $y$ is the profile of the membrane [3], [19]. Since $d \ll L$, the device can be considered as purely one-dimensional, so that the membrane profile can be described by a continuous function $y(x)$ (see Figure 1b). Taking into account that the electric field $\mathbf{E}$ is locally orthogonal to the tangent straight line to the membrane, it can be considered proportional to its curvature $K(x, y(x))$ [24]. Also, because $\frac{\lambda^2}{(1-y(x))^2}$ is proportional to $|\mathbf{E}|^2$ (that is $\frac{d^2y(x)}{dx^2} = -\theta|\mathbf{E}|^2$, $\theta \in \mathbb{R}^+$), we can derive a more realistic model [19], [20]:

$$\begin{cases} \frac{d^2y(x)}{dx^2} = -\frac{1}{\theta\lambda^2}(1 + (\frac{dy(x)}{dx})^2)^3(1 - d^* - y(x))^2 \\ y = 0 \quad \text{on } \partial\Omega \\ y \in C^2([\partial\Omega]), \\ 0 \leq y(x) < 1 - d^* < 1 \\ \frac{d^2y(x)}{dx^2} \in (\overline{\Omega} \times \mathbb{R} \times \mathbb{R}) \end{cases} \quad (2)$$

in which $d^*$ is the distance that separates the top of the membrane profile from the upper plate (critical security distance). As above mentioned, the device is subjected to an external $V$, and thus we have that

$$|\mathbf{E}| \approx \frac{V}{d - y(x)}, \quad (3)$$

which produces an electrostatic pressure

$$p_{el} \approx 0.5\epsilon_0|\mathbf{E}|^2 = 0.5\frac{\epsilon_0 V^2}{(d - y(x))^2}. \quad (4)$$

This results in a mechanical pressure $p = kp_{el}$ ($k$ constant) that deforms the membrane moving towards the upper plate. Under the condition of maximum deformation, the membrane will be at a critical distance of $d^*$ from the upper plate.

### B. WHEN $|\mathbf{E}|$ IS PROPORTIONAL TO $K$
In [19], the model (1) has been studied observing that $\lambda^2 \propto V^2$, and $\frac{\lambda^2}{(1-y(x))^2} \propto |\mathbf{E}|^2$. Accordingly, (1) becomes
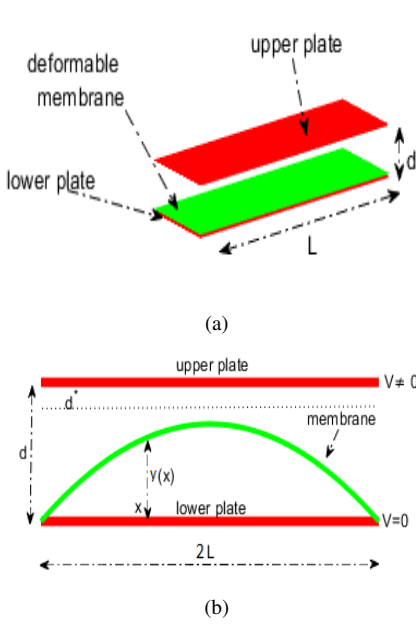
**IEEE** Access



(a)



(b)

FIGURE 1: (a) Electrostatic MEMS device, (b) Typical profile of a MEMS membrane.

$$\begin{cases} \frac{d^2 y(x)}{dx^2} = -\theta |\mathbf{E}|^2 & \text{in } \Omega = [-L_1, L_1] \\ y(-L_1) = y(L_1) = 0 & \theta \in \mathbb{R}^+, \end{cases} \quad (5)$$

where $L_1$ is the half-length of the device. Since $\mathbf{E}$ is locally normal to the tangent straight line of the membrane (see Figure (2)), $|\mathbf{E}|$ results proportional to $K(x, y(x))$, thus we have that [24]

$$K(x, y(x)) = \frac{\left| \frac{d^2 y(x)}{dx^2} \right|}{\sqrt{(1 + (y(x))^2)^3}}, \quad (6)$$

and $|\mathbf{E}|$ can be written as follows:

$$|\mathbf{E}|^2 = (\mu(x, y(x), \lambda))^2 (K(x, y(x)))^2 =$$
$$= \lambda^2 (1 - y(x))^{-2} \left| \frac{d^2 y(x)}{dx^2} \right|^2 (1 + (y(x))^2)^{-3} \quad (7)$$

where $\mu(x, y(x), \lambda) \in C^0([-L_1, L_1] \times [0, 1) \times [\lambda_{\min}, \lambda_{\max}])$ [19].

## III. NUMERICAL APPROACHES

### A. SHOOTING PROCEDURE & ODE SOLVERS

To apply the Shooting procedure, we consider a generic second-order non-linear Boundary Value Problem (BVP) $\frac{d^2 y(x)}{dx^2} = F\left(x, y(x), \frac{dy(x)}{dx}\right)$: recasting it into a system of first order differential equations [21]:

$$\begin{cases} \frac{dy_1(x)}{dx} = y_2 \\ \frac{dy_2(x)}{dx} = F(x, y_1(x), y_2(x)), \end{cases} \quad (8)$$
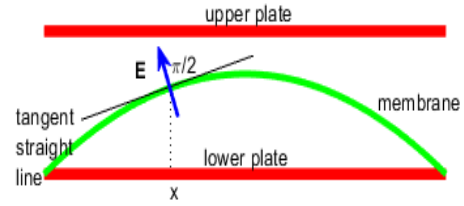


FIGURE 2: The electrostatic membrane MEMS device: $\mathbf{E}$ (blue vector) is orthogonal to the tangent straight line to the membrane so that $|\mathbf{E}|$ can be considered proportional to the curvature of the membrane.

and by setting

$$\begin{cases} y_1(x) = y(x); \\ y_2(x) = \frac{dy_1(x)}{dx} = \frac{dy(x)}{dx}, \end{cases} \quad (9)$$

the original BVP (8) is turned into an Initial Value Problem (IVP) by replacing $y_1(L_1)$ at $x = L_1$ with $y_2(-L_1) = \eta, \eta \in \mathbb{R}$. Now, integrating this last problem, we achieve $y_1(L_1)$ at $x = L_1$. If $y_1(L_1) = 0$ then we have solved the starting BVP, that in this way defines, implicitly, a non-linear equation of the form

$$F(\eta) = y_1(L_1; \eta) = 0 \quad (10)$$

that can be iteratively solved to find the right value of $\eta$ [21].

### 1) Zeros of $F(\eta) = 0$: The Dekker-Brent Procedure

The Dekker's approach exploits the bisection procedure to solve a given non linear equation [22]. For each iteration, three points are involved: $b_k$, which approximates temporary the zero; $a_k$, which is the "contra-point" such that $F(a_k)$ and $F(b_k)$ have opposite sign, so that the interval $[a_0, b_0]$ contains the solution, and $b_{k-1}$, which is the value of $b$ at the previous iteration. Two temporary values are computed: the first one is achieved by the secant procedure, while the second one is obtained by bisection method [21, 22];

$$\begin{cases} s = b_k - \frac{b_k - b_{k-1}}{F(b_k) - F(b_{k-1})} F(b_k) & \text{if } F(b_k) \neq F(b_{k-1}) \\ s = m = \frac{a_k + b_k}{2} & \text{otherwise.} \end{cases} \quad (11)$$

If $s$ (the result of the secant method) is included between $b_k$ and $m$, then $s = b_{k+1}$, otherwise $m = b_{k+1}$. The new value of the contra-point is selected so that $F(a_{k+1})$ and $F(b_{k+1})$ have different sign. In this case $a_{k+1} = a_k$, otherwise, $a_{k+1} = b_k$. Finally, if

$$|F(a_{k+1})| < |F(b_{k+1})|, \quad (12)$$

$a_{k+1}$ turns out to be a best approximation of the solution with respect to $b_{k+1}$, so that $a_{k+1}$ and $b_{k+1}$ are exchanged. However, there are circumstances in which each iteration uses the secants method, but the term $b_k$ converges very slowly. To avoid this problem, Brent proposed a modification of this strategy inserting a test that must be satisfied before the result of the secant method is accepted for the next

IEEE Access

iteration. Given a tolerance $\delta$, if the previous step has been used in the bisection method,

$$|\delta| < |b_k - b_{k-1}| \tag{13}$$

and

$$|\delta| < |s - b_k| < \frac{1}{2}|b_k - b_{k-1}| \tag{14}$$

must be applied to perform the interpolation, otherwise the bisection method is used again. If the previous step used interpolation,

$$|\delta| < |b_{k-1} - b_{k-2}| \tag{15}$$

and

$$|\delta| < |s - b_k| < \frac{1}{2}|b_{k-1} - b_{k-2}| \tag{16}$$

are applied to decide whether to perform the interpolation (when the inequalities are both satisfied) or the bisection (otherwise). This modification ensures that at the $k^{th}$ iteration, the bisection method is used at most for $2\log_2\left(\frac{|b_{k-1}-b_{k-2}|}{\delta}\right)$ times. Furthermore, the Brent method uses inverse quadratic interpolation instead of linear one (as in the secant method). If $F(b_k)$, $F(a_k)$ and $F(b_{k-1})$ are different, the efficiency of the method increases slightly. Consequently, the condition to accept $s$ must be changed: $s$ must be between $\frac{3a_k+b_k}{4}$ and $b_k$.

### 2) Obtaining the Solution
At each iteration $\eta_k$ is obtained by solving the related IVP. A suitable termination criteria have to be used to verify if $\eta_k \to \eta$ as $k \to \infty$. The solutions are obtained by using both teh Matlab built-in functions *ode23* and *ode45* [22, 25], with the accuracy and adaptivity parameters defined by default. We note that the main difficulty to obtain the solutions concerns the fact that the integration of IVPs that sometimes could be not stable. This means that the solutions of the BVP could be insensitive from the variations of the boundary values, while the solutions of the IVP obtained by the Shooting method are computed through the variations of the initial values [26].

### B. RELAXATION PROCEDURE & KELLER-BOX SCHEME
In order to apply the relaxation procedure, we employ a mesh of points $x_0 = -L_1$, $x_j = x_0 + j\Delta x$, for $j = 1, 2, \ldots, J$, evenly spaced with $x_J = L_1$. We denote the numerical approximation to the solution $\mathbf{y}(x_j)$ of (8) by the $2D$ vector $\mathbf{y}_j, j = 0, 1, \ldots, J$ [21, 22]. The Keller Box scheme [27] can be written as follows

$$\begin{cases} \mathbf{y}_j - \mathbf{y}_{j-1} - \Delta\mathbf{F}\left(x_{j-1/2}\frac{\mathbf{y}_j+\mathbf{y}_{j-1}}{2}\right) = \mathbf{0} \\ j = 1, \cdots, J \end{cases} \tag{17}$$

with $\mathbf{G}(\mathbf{y}_0, \mathbf{y}_J) = \mathbf{0}$ and $x_{j-1/2} = (x_j + x_{j-1})/2$. Now, we deal with the system of non-linear equations (17) with respect to the unknown $2(J+1)$-dimensional vector:

$$\mathbf{y} = (\mathbf{y}_0, \mathbf{y}_1, \cdots, \mathbf{y}_J)^T. \tag{18}$$

If $\mathbf{y}(x)$ and $\mathbf{F}(x, \mathbf{y})$ are sufficiently smooth, the solution can be computed by the classical Newton's method, provided

that a sufficiently fine mesh and an accurate initial guess are used. We apply the Newton's method with the following termination criterion [21]

$$\frac{1}{2(J+1)}\sum_{\ell=1}^{2}\sum_{j=0}^{J}|\Delta y_{j\ell}| \leq \mathrm{TOL}, \tag{19}$$

where $\Delta y_{j\ell}$, $j = 0, 1, \ldots, J$ and $\ell = 1, 2$, is the difference between two successive iterate components and $\mathrm{TOL}$ is a fixed tolerance. The adopted initial guess to start the iterations is the following: $y_1(x) = 1$, $y_2(x) = 1$. As far as the accuracy issue is concerned, the truncation error of the method (17) has an asymptotic expansion in powers of $(\Delta x)^2$ [21, 22].

### C. COLLOCATION PROCEDURE & III/IV-STAGE LOBATTO IIIA FORMULAS
#### 1) The Collocation Approach
We consider the following system of ordinary differential equations (ODEs) [21]:

$$\begin{cases} \frac{d\mathbf{y}(r)}{dr} = \mathbf{F}(r, \mathbf{y}(r)) \\ \mathbf{G}[\mathbf{y}(a), \mathbf{y}(b)] = 0 \end{cases} \tag{20}$$

where $\mathbf{G}[\mathbf{y}(a), \mathbf{y}(b)] = 0$ represents the boundary conditions. Converting (20) in an integral equation, we obtain:

$$\mathbf{y}(x) = \mathbf{y}(x_n) + \int_{x_n}^{x}\mathbf{F}(r, \mathbf{y}(r))dr. \tag{21}$$

Replacing $\mathbf{y}(x_n)$ by the approximated value $\mathbf{y}_n$, we can write:

$$\mathbf{y}(x) \approx \mathbf{y}_n + \int_{x_n}^{x}\mathbf{p}(r)dr, \tag{22}$$

in which $\mathbf{p}(r)$ is an interpolation polynomial of degree lower than $s$ interpoling

$$[x_{n,i}, \mathbf{F}(x_{n,i}), \mathbf{y}(x_{n,i})], \quad i = 1, 2, \ldots, s, \tag{23}$$

and

$$x_{n,i} = x_n + \tau_i h, \quad i = 1, \ldots, s, \tag{24}$$
$$0 \leq \tau_1 < \ldots < \tau_s \leq 1.$$

In order to evaluate this polynomial it is possible to exploit the Lagrange or the Newton interpolation polynomial technique [22]. If Lagrange method is exploited, we can write:

$$\mathbf{p}(r) = \sum_{j=1}^{s}\mathbf{F}(x_{n,j}, \mathbf{y}(x_{n,j}))\mathbf{L}_j(r), \tag{25}$$

where $\mathbf{L}_j(r)$ are the fundamental Lagrange polynomials [21, 22]. Then, plugging (25) into (22) we obtain:

$$\mathbf{y}(x) \approx \mathbf{y}_n + \sum_{j=1}^{s}\mathbf{F}(x_{n,j}, \mathbf{y}(x_{n,j}))\int_{x_n}^{x}\mathbf{L}_j(r)dr. \tag{26}$$

4

Then, (26) is forced for all the $x_{n,j}$, so that $\mathbf{y}_{n,j}$ at collocation node points are obtained, for $i = 1, ..., s$, by:

$$\mathbf{y}_{n,j} = \mathbf{y}_n + \sum_{j=1}^{s} \mathbf{F}(x_{x_{n,i}}, \mathbf{y}_{n_{n,j}}) \int_{x_n}^{x_{n,i}} \mathbf{L}_j(r)dr. \quad (27)$$

If $\tau_s = 1$,

$$\mathbf{y}_{n+1} = \mathbf{y}_{n,s}, \quad (28)$$

otherwise:

$$\mathbf{y}_{n+1} = \mathbf{y}_n + \sum_{j=1}^{s} \mathbf{F}(x_{n,j}, \mathbf{y}_{n,j}) \int_{x_n}^{x_{n+1}} \mathbf{L}_j(r)dr. \quad (29)$$

Collocation methods are reliable tools, although may not be suitable if high accuracy is required [21].

### 2) Implicit Runge-Kutta Procedures

Runge-Kutta (RK) methods involve many evaluations of the function $\mathbf{F}(x, \mathbf{y}(x))$ in each interval $[x_n, x_{n+1}]$. In its more general form, an RK method can be written in the following way [22]:

$$y_{n+1} = y_n + h \sum_{i=1}^{s} b_i k_i \quad (30)$$

where

$$k_i = \mathbf{F}\left( x_n + c_i h, y_n + h \sum_{j=1}^{s} a_{ij} k_j \right), \quad i = 1, 2, ..., s \quad (31)$$

where $s$ denotes the number of stage of the procedure. Coefficients $\{a_{ij}\}$, $\{ci\}$ and $\{b_i\}$ characterize a RK procedure and can be collected in the Butcher Tableau [21, 22]

$$\begin{array}{c|c} \mathbf{c} & A \\ \hline & \mathbf{b}^T \end{array} \quad (32)$$

where $A = (a_{ij}) \in \mathbb{R}^{s \times s}$, $\mathbf{b} = (b_1, ..., b_s)^T \in \mathbb{R}^s$ and $\mathbf{c} = (c_1, ..., c_s)^T \in \mathbb{R}^s$. IF coefficients $a_{ij}$ are equal to zero for $j \geq i$, with $i = 1, 2, ..., s$, then each $k_i$ can be explicitly computed exploiting the $i-1$ coefficients $k_1...k_{i-1}$ which have already been calculated. Then, RK procedure is called explicit. Otherwise, it is said implicit. and to compute the coefficient $k_i$ one has solve a $s$-dimensional non-linear system. To construct an implicit RK methods one needs to consider three conditions as follows [21]:

$$B(p) : \sum_{i=1}^{s} b_i c_i^{k-1} = k^{-1}, \quad k = 1, 2, ..., p \quad (33)$$

$$C(q) : \sum_{i=1}^{s} a_{ij} c_i^{k-1} = k^{-1} c_i^k, \quad (34)$$
$$k = 1, 2, ..., p, \quad i = 1, 2, ..., s$$

$$D(r) : \sum_{i=1}^{s} b_i c_i^{k-1} a_{ij} = k^{-1} b_j (1 - c_j^k), \quad (35)$$
$$k = 1, 2, ..., r, \quad j = 1, 2, ..., s.$$

Condition (33) means that the following quadrature formula

$$\int_x^{x+h} \mathbf{F}(s)ds \approx h \sum_{i=1}^{s} b_i \mathbf{F}(x + c_i h) \quad (36)$$

is exact for all polynomials whose degree is lower than $p$. If (33) is satisfied, then the RK method has quadrature of order $q$. Analogously for condition (34). In other words, if it is satisfied, then the corresponding quadratures

$$\int_x^{t+c_i h} \mathbf{F}(s)ds \approx h \sum_{j=1}^{s} a_{ij} \mathbf{F}(x + c_j h) \quad (37)$$

are exact for all polynomials whose degree are lower than $q$. In this case the RK procedure is of stage of order $q$. It is proved that all methods satisfying condition (34) having $c_i$, $i = 1, 2, ..., s$ distinct are collocation procedures.

In order to simplify the construction of an implicit Runge-Kutta procedure, one can exploit the following well-known Lemma [21, 22].

*Lemma 1:* Let us consider a RK procedure with $s$ stage having $c_1 \neq c_2 \neq ... \neq c_s$. In addition, let be $b_j$, $j = 1, 2, ..., s$. Then, the two following statements occurs:
1. $C(s) \wedge B(s + \nu) \Rightarrow D(\nu)$
2. $D(s) \wedge B(s + \nu) \Rightarrow C(\nu)$
so that one ca built the procedure exploiting $B(p)$ and $D(r)$ or $C(q)$.

### 3) The Three-stage Lobatto IIIa Formula

This procedure requires that the coefficient $c_i$ must be chosen as roots of [21]:

$$P_s^* - P_{s-2}^* = \frac{d^{s-2}}{dx^{s-2}}(x^{s-1}(x-1)^{s-1}), \quad (38)$$

where $s$ is the number of the stage, obtaining in this way $c_1 = 0$ and $c_s = 1 \, \forall s$, so that the quadrature formula is exact for any polynomial whose degree is less than $2s - 2$ [28]. Let us premise the following two definitions.

*Definition 1:* (definition of the step-size)
Let us consider the following mesh-grid:

$$0 = a = r_0 < r_1 < ... < r_n = b = R \quad (39)$$

and, on it, let us define the step-size $h_m = r_{m+1} - r_m$.

*Definition 2:* (midpoint and approximation at the midpoint)
Starting from $(r_m, r_{m-1})$, we denote their midpoints by $r_{m+1/2}$ and by $y_{m+1/2}$ the approximation of $y(r)$ at $r_{m+1/2}$.

*Remark 1:* (On the order of the polynomial) The cubic polynomial $\mathbf{p}(r)$ satisfy the boundary conditions in (20) and, in addition, $\forall(r_m, r_{m+1})$, the subdivision (39) is taken into account. In addition, $\mathbf{p}(r)$ is located at the edges of each subinterval and midpoint as well where $\mathbf{p}(r)$ is continuous.

**IEEE** *Access*

This approach is a collocation procedure and it is proved that is totally equivalent to the three-stage Lobatto IIIa implicit RK procedure [28] whose Butcher tableau is [21]

$$
\begin{array}{c|ccc}
0 & 0 & 0 & 0 \\
\frac{1}{2} & \frac{5}{24} & \frac{1}{3} & -\frac{1}{24} \\
1 & \frac{1}{6} & \frac{2}{3} & \frac{1}{6} \\
\hline
& \frac{1}{6} & \frac{2}{3} & \frac{1}{6}
\end{array}
\tag{40}
$$

Then, the three-stage Lobatto IIIa formula can be written as follows [21]:

$$
\mathbf{y}_{m+1/2} = \mathbf{y}_m + h_m \left[ \frac{5}{24}\mathbf{F}(r_m, \mathbf{y}_m) + \right. \tag{41}
$$

$$
\left. + \frac{1}{3}\mathbf{F}(r_{m+1/2}, \mathbf{y}_{m+1/2}) - \frac{1}{24}\mathbf{F}(r_{m+1}, \mathbf{y}_{m+1}) \right]
$$

$$
\mathbf{y}_{m+1} = \mathbf{y}_m + h_m \left[ \frac{1}{6}\mathbf{F}(r_m, \mathbf{y}_m) + \right. \tag{42}
$$

$$
\left. + \frac{2}{3}\mathbf{F}(r_{m+1/2}, \mathbf{y}_{m+1/2}) + \frac{1}{6}\mathbf{F}(r_{m+1}, \mathbf{y}_{m+1}) \right].
$$

*Remark 2 (on the use of Simpson quadrature formula):* This procedure can be derived from the (21) exploiting the Simpson quadrature formula to approximate the integral between $x_n$ and $x$. Obviously, when the procedure is applied to a quadrature problem, it reduces (42) to the well-known Simpson formula [22]:

$$
\mathbf{y}_{m+1} = \mathbf{y}_m + \frac{h_m}{6} \left[ \mathbf{F}(r_m, \mathbf{y}_m) + \right. \tag{43}
$$

$$
+ \mathbf{F}(r_{m+1}, \mathbf{y}_{m+1}) + 4\mathbf{F} \left\{ r_{m+1/2}, \frac{\mathbf{y}_{m+1} + \mathbf{y}_m}{2} + \right.
$$

$$
\left. \left. + \frac{h_m}{8} \left[ \mathbf{F}(r_m, \mathbf{F}(r_m, \mathbf{y}_m) - \mathbf{F}(r_{m+1}, \mathbf{y}_{m+1}) \right] \right\} \right].
\tag{44}
$$

*Remark 3 (on the polynomial $\mathbf{p}(r)$ and its derivatives: collocation polynomial):* We note that $\mathbf{p}(r)$ and their derivaties satisfy, $\forall r \in (a, b)$ [28],

$$
\mathbf{p}^{(l)}(r) = \mathbf{y}^{(l)}(r) + \mathcal{O}(h^{4-l}), \quad l = 0, 1, 2, 3. \tag{45}
$$

Furthermore, equations (20) are satisfied by $\mathbf{p}(r)$ at each intermediate point and at the midpoint of each interval as well (collocation polynomial). It is worth nothing that the form of $\mathbf{p}(r)$ is chosen by Matlab by means of the determination of unknown parameters, if any. Finally, we can write:

$$
\begin{cases}
\mathbf{p}'(r_m) = \mathbf{F}[r_m, \mathbf{p}(r_m)] \\
\mathbf{p}'(r_{m+1/2}) = \mathbf{F}[r_{m+1/2}, \mathbf{p}(r_{m+1/2})], \\
\mathbf{p}'(r_{m+1}) = \mathbf{F}[r_{m+1}, \mathbf{p}(r_{m+1})]
\end{cases}
\tag{46}
$$

which represent non-linear equations that can be solved by a Matlab solver. Moreover, Matlab, $\forall r \in (a, b)$, evaluates the cubic polynomial by means of its special function *bvpval* [25].

*Remark 4 (a guess for the solution & initial mesh):* It is known that a BVP could have more than one solution [22]. Then, it is important to supply a guess for both the initial mess and the solution as well. Obviously, the Matlab solver adapt the mesh obtaining a solution by means of a reduced number of mesh points [25].

It is worth noting that, very often, a good initial hypothesis is extremely complicated. Then, the Matlab solver acts by checking a residue defined as [25]:

$$
\mathbf{res}(r) = \mathbf{p}'(r) - \mathbf{F}[r, \mathbf{p}(r)]. \tag{47}
$$

while the boundary conditions become $\mathbf{g}[\mathbf{p}(a), \mathbf{p}(b)]$. Obviously, if $\mathbf{res}(r)$ is small, then $\mathbf{p}(r)$ represents a good solution and, in the case of well-conditioned problem, $\mathbf{p}(r)$ is close to $\mathbf{y}(r)$. In this paper, the the Matlab R2017a *bvp4c* solver has been exploited because, firstly, it implements the collocation technique by means of a piecewise cubic $\mathbf{p}(r)$, whose coefficients are determined requiring that $\mathbf{p}(r)$ be continuous on $(a, b)$. Moreover, both mesh and estimation error are based on the evaluation of the residual of $\mathbf{p}(r)$ whose control is useful to manage poor or inadequate guesses for both mesh and solution [25]. In addition, this Toolbox presents a very reduced computational complexity to achieve the Jacobian

$$
J = \frac{\partial F_i}{\partial \mathbf{y}} = \begin{bmatrix} \frac{\partial F_1}{\partial y_1} & \frac{\partial F_1}{\partial y_2} \\ \frac{\partial F_2}{\partial y_1} & \frac{\partial F_2}{\partial y_2} \end{bmatrix}. \tag{48}
$$

Finally, being *bvp4c* a vectorized solver, it is able to strongly reduce the run-time vectorizing $\mathbf{F}(r, \mathbf{y}(r))$ [25].

#### 4) Four-stage Lobatto IIIa Formula

This formula is derived as an implicit RK procedure whose Butcher tableau is the following [21]:

$$
\begin{array}{c|cccc}
0 & 0 & 0 & 0 & 0 \\
\frac{5-\sqrt{5}}{10} & \frac{11+\sqrt{5}}{120} & \frac{25-\sqrt{5}}{120} & \frac{25-13\sqrt{5}}{120} & \frac{-1+\sqrt{5}}{120} \\
\frac{5+\sqrt{5}}{10} & \frac{11-\sqrt{5}}{120} & \frac{25+13\sqrt{5}}{120} & \frac{25+\sqrt{5}}{120} & \frac{-1-\sqrt{5}}{120} \\
1 & \frac{1}{12} & \frac{5}{12} & \frac{5}{12} & \frac{1}{12} \\
\hline
& \frac{1}{12} & \frac{5}{12} & \frac{5}{12} & \frac{1}{12}
\end{array}
\tag{49}
$$

As the three-stage formula, this approach is a polynomial collocation procedure providing solutions belonging to the space $C^1([a, b])$ with accuracy of the fifth-order. Unlike the *bvp4c* solver that exploits analytical condensation procedure, Matlab solves the four-stage Lobatto IIIA formula by finite difference approach (*bvp5c* solver) and solves the algebraic equations directly. Moreover, unlike *bvp4c* solver that handles the unknown parameters directly, *bvp5c* solver augments the system with trivial differential equations for unknown parameters [21, 22, 25].
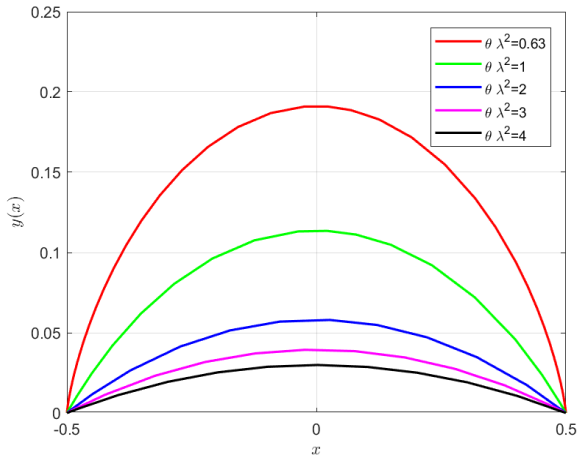
FIGURE 3: Profile of the membrane $y(x)$ for different values of $\theta\lambda^2$ when the shooting procedure & *ode23* ToolBox Matlab is exploited. The deflection of the membrane increases when $\theta\lambda^2$ decreases.

## IV. NUMERICAL RESULTS

In this section, we present the numerical results obtained by using the numerical procedures discussed in the previous section. At this purpose, we rewrite (2) as a system of first order ODEs, and applying (8) and (9), we can write:

$$\begin{cases} \frac{dy_1(x)}{dx} = y_2(x) \\ \frac{dy_2(x)}{dx} = -\frac{1}{\theta\lambda^2}(1+y_2^2(x))^3(\alpha-y_1(x))^2, \\ y_1(-L_1) = y_1(L_1) = 0 \end{cases} \quad (50)$$

*Remark 5:* It is worth nothing that if $y(x) = 1 - d^*$, from the model (2) it can be seen that $\frac{d^2y(x)}{dx^2} = 0$. In other words, this condition has no physical relevance because from the model (1) (or model (5)) we would supply $|\mathbf{E}| = 0$ with linear deflection of the membrane.

Figure 3 shows the numerical results for the membrane profile $y(x)$ computed by using different values of the parameter $\theta\lambda^2$ exploiting the Shooting method implemented by the Matlab built-in function *ode23*. It can be noted that the minimum value of this parameter that guarantees the convergence of the procedures is equal to $\theta\lambda^2 = 0.63$. Similar results are obtained by applying the other numerical approaches. For all computation, we choose $d^* = 10^{-4}$ and $L_1 = 0.5$. For the Shooting method & ODE solvers (Shoot&23 and Shoot&45), we set $y_1(0) = 1$ and $y_2(0) = 1.2$ as initial guess for $\theta\lambda^2 = 0,63,1,4$ and $y_1(0) = 0.1$ and $y_2(0) = 0.2$ as initial guess for $\theta\lambda^2 = 2,3$. For the relaxation procedure & Keller box scheme (Rel&Box), we set both initial guesses as $y_1(0) = y_2(0) = 1$. Finally, $y_1(0) = y_2(0) = 0$ are set for the collocation procedure & Lobatto formulae (Col&III and Col&IV). A comparison of the results obtained for values of $\theta\lambda^2 = 0.63,1,2,3$ is reported in Table 1. Finally, with $\theta\lambda^2 = 4$, we obtain the same value $\max(y(x)) = 0.029918$, for a number of

TABLE 1: Comparison of the results for different values of the parameter $\theta\lambda^2$.

| Methods | $\theta\lambda^2 = 0.63$ | | $\theta\lambda^2 = 1$ | |
|---|---|---|---|---|
| | $\max(\mathbf{y}(\mathbf{x}))$ | **J** | $\max(\mathbf{y}(\mathbf{x}))$ | **J** |
| Shoot&23 | 0.190943 | 64 | 0.113476 | 20 |
| Shoot&45 | 0.189749 | 364 | 0.113639 | 56 |
| Rel&Box | 0.191257 | 4000 | 0.113662 | 4000 |
| Col&III | 0.189623 | 44 | 0.113653 | 12 |
| Col&IV | 0.190331 | 40 | 0.113662 | 10 |
| Methods | $\theta\lambda^2 = 2$ | | $\theta\lambda^2 = 3$ | |
| | $\max(\mathbf{y}(\mathbf{x}))$ | **J** | $\max(\mathbf{y}(\mathbf{x}))$ | **J** |
| Shoot&23 | 0.057973 | 14 | 0.039371 | 14 |
| Shoot&45 | 0.058133 | 52 | 0.039432 | 52 |
| Rel&Box | 0.058133 | 4000 | 0.039452 | 4000 |
| Col&III | 0.058124 | 4 | 0.039451 | 4 |
| Col&IV | 0.058133 | 6 | 0.039452 | 4 |

grid points equal to $J = 14,52,4000,4,6$, respectively. The numerical results demonstrate that each numerical procedure considered in this study shows an excellent performance in recovering the membrane profile. However, it can be noticed as the profile is computed exploiting for each method a different order of accuracy and a different number of grid points. We have that both the relaxation method and the Keller box scheme reveals robust and accurate. Notably, the Keller box provides results as accurate as those of the Shooting and collocation method, because it involves more grid points are for its computations. However, because of that, it is slower and has a higher computational cost than these methods. The Shooting method is not as robust as the relaxation and the collocation methods, but it has the advantage of the speed and adaptivity of the Matlab built-in functions *ode23* and *ode45*, that have been used for solving the related IVPs. Finally, the collocation method provides a solution by using very few numbers of grid points. This because the profile is not characterized by hardly sharp changes. Now, although all the considered numerical approaches represent efficient and reliable tools for solving the BVPs in the case of convergence conditions ensuring the absence of ghost solutions, we can conclude that the relaxation approach and the Keller box scheme reveals more robust in all performed numerical tests.

## V. CONVERGENCE OF THE NUMERICAL APPROACHES

Indicating by $[(\theta\lambda^2)_{conv}]_{S_{ode23}}$ the range of $\theta\lambda^2$ ensuring convergence by means of shooting procedure exploiting *ode23* Matlab®, in [23] it was experimentally achieved that

$$[(\theta\lambda^2)_{conv}]_{S_{ode23}} = [0.63, +\infty) \quad (51)$$

so that if

$$[(\theta\lambda^2)_{no\,conv}]_{S_{ode23}} = [0, 0.63) \quad (52)$$

the convergence of the numerical procedure is not ensured. In addition, exploiting the Keller-Box scheme, in [26], the experimental range of $\theta\lambda^2$ ensuring convergence was

$$[(\theta\lambda^2)_{conv}]_{Keller-Box} = [0.592, +\infty). \quad (53)$$

Also in this case, if

$$[(\theta\lambda^2)_{no\,conv}]_{Keller-Box} = [0, 0.592) \quad (54)$$

**IEEE** *Access*

the convergence of the Keller-Box scheme procedure is not ensured. In this paper, the experimental range of $\theta\lambda^2$ ensuring convergence when the Shooting procedure exploiting *ode45* Matlab® is applied, has been achieved. In particular, as for Shooting with *ode23* MatLab®

$$[(\theta\lambda^2)_{conv}]_{S_{ode45}} = [0.63, +\infty) \quad (55)$$

and the range that does not ensure convergence, for this case, is:

$$[(\theta\lambda^2)_{no\,conv}]_{S_{ode45}} = [0, 0.63). \quad (56)$$

Finally, applying both Three and Four Stage Lobatto IIIa Formulas we have experimentally achieved

$$[(\theta\lambda^2)_{conv}]_{ThreeStage_{Lobatto}} = [1.181, +\infty) \quad (57)$$

and

$$[(\theta\lambda^2)_{conv}]_{FourStage_{Lobatto}} = [1.181, +\infty) \quad (58)$$

so that, for both Three and Four Stage Lobatto IIIa Formulas, the range of $\theta\lambda^2$ that does not ensure the convergence is:

$$[(\theta\lambda^2)_{noconv}]_{FourStage_{Lobatto}} = [0, 1.181). \quad (59)$$

Table 2 summarizes these conditions. In the event that all numerical procedures worked in parallel, we are interested in knowing the minimum value of $\theta\lambda^2$ above which the convergence of at least one numerical procedure is guaranteed. Then, the following makes sense:

$$\min(\theta\lambda^2)_{conv} = \quad (60)$$
$$= \min\left\{\min[(\theta\lambda^2)_{conv}]_{S_{ode23}},\right.$$
$$\min[(\theta\lambda^2)_{conv}]_{Keller-Box},$$
$$\min[(\theta\lambda^2)_{conv}]_{S_{ode45}},$$
$$\min[(\theta\lambda^2)_{conv}]_{ThreeStage_{Lobatto}},$$
$$\left.\min[(\theta\lambda^2)_{conv}]_{FourStage_{Lobatto}}\right\} = 0.592.$$

In other words, for values greater than or equal to $0.592$ the convergence of at least one numerical solution is guaranteed. Accordingly, for $\theta\lambda^2 \geq 0.63$ the convergence is guaranteed for all the methods. However, we point out that even if a numerical solution is obtained, we must be sure that this satisfy the analytical condition of existence and uniqueness for (2) if we want to avoid the possibility of evaluating a potential ghost solution.

## VI. EXISTENCE AND UNIQUENESS OF THE SOLUTION DEPENDING ON THE ELECTROMECHANICAL PROPERTIES OF THE MEMBRANE.

In [19] the problem of the existence and uniqueness of the solution for (2) has been studied demonstrating that: *i)* the uniqueness is always guaranteed, and that *ii)* the existence conditions take the form:

$$1 + \left(\sup\left\{\left|\frac{dy(x)}{dx}\right|\right\}\right)^6 <$$
$$< 0.5(\alpha L_1)^{-1}\left(\sup\left\{\left|\frac{dy(x)}{dx}\right|\right\}\right)\theta\overline{\lambda}^2 \quad (61)$$

TABLE 2: For each exploited numerical procedure, the ranges of $\theta\lambda^2$ ensuring convergence.

| | | |
|---|---|---|
| **Shooting** (*ode23*) | $\theta\lambda^2 \in [0.63, +\infty)$ convergence | $\theta\lambda^2 \in [0, 0.63)$ no convergence |
| **Shooting** (*ode45*) | $\theta\lambda^2 \in [0.63, +\infty)$ convergence | $\theta\lambda^2 \in [0, 0.63)$ no convergence |
| **Keller-Box** | $\theta\lambda^2 \in [0.592, +\infty)$ convergence | $\theta\lambda^2 \in [0, 0.592)$ no convergence |
| **Three Stage Lobatto IIIa** (*bvp4c*) | $\theta\lambda^2 \in [1.181, +\infty)$ convergence | $\theta\lambda^2 \in [0, 1.181)$ no convergence |
| **Four Stage Lobatto IIIa** (*bvp5c*) | $\theta\lambda^2 \in [1.181, +\infty)$ convergence | $\theta\lambda^2 \in [0, 1.181)$ no convergence |

where the parameter $\overline{\lambda}^2$ depends by the minimum value of the applied voltage $V$ needed to overcome the membrane inertia. Moreover, in [19], it was demonstrated that:

$$\sup\left\{\left|\frac{dy(x)}{dx}\right|\right\} = 99. \quad (62)$$

*Remark 6:* It is worth noting that $\sup\{|\frac{dy(x)}{dx}|\} = 99$ is quite high. This is due to the fact that a large number of increases were necessary to obtain the condition (61). In any case, the value obtained, albeit high, is certainly a safety advantage.

*Remark 7:* It is also observable that, in [19], the uniqueness of the solution for the (2) problem is always guaranteed. However, the proof, using the joint use of Poincaré inequality and the Gronwall Lemma, did not highlight behaviors dependent on the electromechanical characteristics of the material constituting the membrane. In other words, uniqueness was always guaranteed regardless of the material constituting the membrane.

In what follows, we present a new condition that links the uniqueness of the solution for (2) to the electromechanical properties of the MEMS membrane:

*Theorem 1:* Let us consider problem (2). If

$$1 + \left(\sup\left\{\left|\frac{dy(x)}{dx}\right|\right\}\right)^6 < (24L_1(L_1+1))^{-1}\theta\lambda^2 \quad (63)$$

then (2) admits unique solution.
*Proof*: see appendix.

Finally, in order to achieve a unique condition that ensures both existence and uniqueness, we have to solve the following system:

$$\begin{cases} 1 + \left(\sup\left\{\left|\frac{dy(x)}{dx}\right|\right\}\right)^6 < \\ < 0.5(\alpha L_1)^{-1}\theta\overline{\lambda}^2\left(\sup\left\{\left|\frac{dy(x)}{dx}\right|\right\}\right) \\ 1 + \left(\sup\left\{\left|\frac{dy(x)}{dx}\right|\right\}\right)^6 < \\ < (6L_1(L_1+1))^{-1}\theta\lambda^2 \ . \end{cases} \quad (64)$$

The system (64) is equivalent to (63). This last relation is of paramount importance because it reduces the risk to compute ghost solutions.

## VII. CONVERGENCE & GHOST SOLUTIONS

Taking into account that $L_1 = 0.5$, from (63) and (62), we obtain that $\theta\lambda^2 \geq 18$ so that if $\theta\lambda^2 \in [18, +\infty)$ we have that both existence and uniqueness for (2) are ensured. Moreover, it is known that [19]:

$$\lambda^2 = \frac{\epsilon_0 L_1^2 V^2}{d^3 T} < \frac{\epsilon_0 L_1^2 V^2}{(1-d^*)^3 T}. \tag{65}$$

Multiplying the above relation for $\theta$, we obtain:

$$\theta\lambda^2 < \frac{\theta\epsilon_0 L_1^2 V^2}{(1-d^*)^3 T}. \tag{66}$$

Combining (63) and (66), we can write:

$$1 + \left(\sup\left\{\left|\frac{dy(x)}{dx}\right|\right\}\right)^6 < \frac{\theta\lambda^2}{24L_1(1+L_1)} \leq$$
$$\leq \frac{\theta\epsilon_0 L_1^2 V^2}{24L_1(1+L_1)(1-d^*)^3 T}, \tag{67}$$

from which:

$$24L_1(1+L_1)\left(\left(\sup\left\{\left|\frac{dy(x)}{dx}\right|\right\}\right)^6\right) <$$
$$\leq \theta\lambda^2 \leq \frac{\theta\epsilon_0 L_1^2}{(1-d^*)^3 T}. \tag{68}$$

But noting that:

$$0.63 \ll 24L_1(1+L_1)\left(1 + \left(\sup\left\{\left|\frac{dy(x)}{dx}\right|\right\}\right)^6\right) \tag{69}$$

we obtain:

$$0.63 \ll$$
$$\ll 24L_1(1+L_1)\left(1 + \left(\sup\left\{\left|\frac{dy(x)}{dx}\right|\right\}\right)^6\right) <$$
$$< \theta\lambda^2 \leq \frac{\theta\epsilon_0 L_1^2 V^2}{(1-d^*)^3 T}, \tag{70}$$

from which:

$$V > \sqrt{\frac{0.63(1-d^*)^3}{\underbrace{\theta\epsilon_0 L_1^2}_{Z1}}}\sqrt{T} = Z_1\sqrt{T}. \tag{71}$$

This last relation highlights that thicker the membrane, the higher the voltage $V$ to be applied to the device for overcoming the inertia of the membrane itself. In addition, since:

$$18 \ll 24L_1(1+L_1)\left(1 + \left(\sup\left\{\left|\frac{dy(x)}{dx}\right|\right\}\right)^6\right), \tag{72}$$
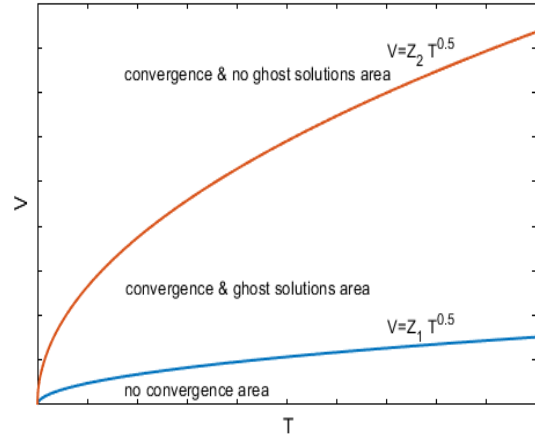
we can write:



FIGURE 4: $T - V$ plane partitioned into three distinct areas: non-convergence area; convergence with ghost solutions area; convergence without ghost solutions area.

$$V > \sqrt{\frac{18(1-d^*)^3}{\underbrace{\theta\epsilon_0 L_1^2}_{Z2}}}\sqrt{T} = Z_2\sqrt{T}, \tag{73}$$

so that both (71) and (73) identify, the plane formed by the mechanical tension $T$ and the applied external voltage V, areas of convergence in the presence/absence of ghost solutions. As shown in Figure 4, (71) defines the non-convergence area for each numerical procedure (area below the blue curve). On the other hand, between the blue and red curves, the convergence is of at least one numerical procedure is highlighted, but the absence of ghost solutions is not guaranteed. Finally, above the red curve, the area where both convergence and absence of ghost solution are guaranteed is highlighted.

*Remark 8:* We note that ensuring the absence of ghost solutions is very important for MEMS devices. This is because it allows, on the one hand, to recover membrane profiles compatible with the geometry of the device and, on the other, to obtain ranges of possible values for $V$, $|\mathbf{E}|$ and $T$ able to define with sufficient rigor operating conditions to which the device must be subjected.

## VIII. RANGE OF PARAMETERS FOR THE CORRECT USE OF THE DEVICE

As previously described, MEMS devices subjected to external $V$ force the membrane to deform towards the upper plate. Therefore, it seems natural to ask, once the material constituting the membrane (ie, fixed $T$) has been chosen, what the range of possible values must be for $V$ and $|\mathbf{E}|$ able to obtain membrane profiles compatible with the device geometry. Vice versa, having fixed the intended use of the device (i.e. fixed $V$ and $|\mathbf{E}|$), we also ask which material

**IEEE** *Access*

is most suitable for building the membrane. With this aim in mind, starting from (63) and (66), and considering that $L_1 = 0.5$, we can easily write:

$$1 + \left( \sup\left\{ \left| \frac{dy(x)}{dx} \right| \right\} \right)^6 < \frac{\theta \lambda^2}{18} =$$
$$= \frac{\theta}{18} \frac{\epsilon_0 L_1^2 V^2}{d^3 T} < \frac{\theta}{18} \frac{\epsilon_0 L_1^2 V^2}{(1-d^*)^3 T}, \qquad (74)$$

from which:

$$\left( \sup\left\{ \left| \frac{dy(x)}{dx} \right| \right\} \right) < \sqrt[6]{ \frac{\theta}{18} \frac{\epsilon_0 L_1^2 V^2}{(1-d^*)^3 T} - 1 }, \qquad (75)$$

that provides the range of admissible values of $\sup\left\{ \left| \frac{dy(x)}{dx} \right| \right\}$, once known *i)* the electromechanical properties of the membrane ($\theta$), *ii)* the lower plate mechanical tension $T$ for $V = 0$, and *iii)* the applied voltage $V$. Moreover, we can write:

$$\theta |\mathbf{E}|^2 = \frac{\lambda^2}{(1-y(x))^2} = \frac{1}{(1-y(x))^2} \frac{\epsilon_0 L_1^2 V^2}{d^3 T} <$$
$$< \frac{1}{(1-y(x))^2} \frac{\epsilon_0 L_1^2 V^2}{(1-d^*)^3 T}. \qquad (76)$$

In addition being $1 - y(x) > 1 - d^*$, we have that $\frac{1}{(1-y(x))^2} < \frac{1}{(1-d^*)^2}$ from which the condition (76) becomes:

$$\theta |\mathbf{E}|^2 < \frac{\epsilon_0 L_1^2 V^2}{(1-d^*)^5 T}, \qquad (77)$$

finally obtaining

$$\frac{|\mathbf{E}|}{V} = \sqrt{ \frac{\epsilon_0 L_1^2}{(1-d^*)^5 T \theta} }. \qquad (78)$$

By (78), fixing the electromechanical properties of the membrane $\theta$ and the mechanical tension $T$, we obtain the ratio between $|\mathbf{E}|$ and $V$, which are the operative electrostatic parameters of the device. Vice versa, starting from (77), we can also write:

$$T\theta < \frac{\epsilon_0 L_1^2 V^2}{(1-d^*)^5 |\mathbf{E}|^2}, \qquad (79)$$

so that, starting from the knowledge of the couple ($|\mathbf{E}|$, $V$), we obtain $T\theta$.

## IX. CONCLUSIONS

In order to recover the membrane profile of a $1D$ model of an electrostatic membrane MEMS device, in which $|\mathbf{E}|$ is locally proportional to the membrane curvature, in this work the Shooting procedure, the Relaxation scheme, and the Collocation technique, have been exploited. Numerical results have highlighted a better performance of the Relaxation & Keller-Box method compared to Shooting procedure and the Lobatto formulas. However, although the relaxation procedure offers the best performance, it requires a higher

computational time (a large number of grid points) than the other approaches. Also, we have determined in the plane formed by the mechanical tension $T$ and the applied external voltage V, the areas where the numerical procedures can converge with or without these being affected by possible ghost solutions. Finally, a new condition of existence and uniqueness, which depends on the device geometry and the electromechanical properties of the membrane, has been obtained. To conclude, we point out that, despite the differential model considered in this work results being simplified in some aspects, the obtained numerical results provide sufficient qualitative pieces of information to analyze MEMS device characterized by simple geometry. Anyway, to improve its adherence to the experimental ones, it appears of paramount importance to improve the MEMS differential model considered in the present study, taking into account more sophisticated geometrical curvature formulations.

## APPENDIX. PROOF OF THEOREM 1
Let us consider two different solutions $y_1(x), y_2(x) \in P$, where:

$$P = \Big\{ C_0^2(\Omega): \ 0 < y(x) < \alpha,$$
$$\left| \frac{dy(x)}{dx} \right| < \sup\left\{ \left| \frac{dy(x)}{dx} \right| \right\} < +\infty \Big\}. \qquad (80)$$

The proof of the Theorem is divided into three steps:
Step 1. We prove that

$$\left| \left(1 + \left(\frac{dy_2(x)}{dx}\right)^2\right)^3 - \left(1 + \left(\frac{dy_1(x)}{dx}\right)^2\right)^3 \right| \le$$
$$\le 24 \left( \sup\left\{ \left| \frac{dy(x)}{dx} \right| \right\} \right)^5 \left| \frac{dy_2(x)}{dx} - \frac{dy_1(x)}{dx} \right|. \qquad (81)$$

In fact, considering that $\sup\left\{ \left| \frac{dy(x)}{dx} \right| \right\} > 1$, we can write:

$$\left| \left(1 + \left(\frac{dy_2(x)}{dx}\right)^2\right)^3 - \left(1 + \left(\frac{dy_1(x)}{dx}\right)^2\right)^3 \right| =$$
$$= \left| \left[ \left(\frac{dy_2(x)}{dx}\right)^2 - \left(\frac{dy_1(x)}{dx}\right)^2 \right] \right.$$
$$\left[ \left(1 + \left(\frac{dy_1(x)}{dx}\right)^2\right)^2 + \left(1 + \left(\frac{dy_2(x)}{dx}\right)^2\right) \right.$$
$$\left. \left(1 + \left(\frac{dy_1(x)}{dx}\right)^2\right) + \left(1 + \left(\frac{dy_2(x)}{dx}\right)^2\right)^2 \right] \right| \le$$
$$\le 2 \left( \sup\left\{ \left| \frac{dy(x)}{dx} \right| \right\} \right) \left| \frac{dy_2(x)}{dx} - \frac{dy_1(x)}{dx} \right|$$
$$\left[ \left(1 + \left( \sup\left\{ \left| \frac{dy(x)}{dx} \right| \right\} \right)^2\right)^2 + \right.$$
$$+ \left(1 + \left( \sup\left\{ \left| \frac{dy(x)}{dx} \right| \right\} \right)^2\right) \right)$$
$$\left(1 + \left( \sup\left\{ \left| \frac{dy(x)}{dx} \right| \right\} \right)^2\right) +$$
$$\left. + \left(1 + \left( \sup\left\{ \left| \frac{dy(x)}{dx} \right| \right\} \right)^2\right)^2 \right] =$$
$$= 2 \left( \sup\left\{ \left| \frac{dy(x)}{dx} \right| \right\} \right) \left| \frac{dy_2(x)}{dx} - \frac{dy_1(x)}{dx} \right|$$

$$\left| \left(1 + \left(\sup\left\{\left|\frac{dy(x)}{dx}\right|\right\}\right)^2\right)^2 + \right.$$
$$+ \left(1 + \left(\sup\left\{\left|\frac{dy(x)}{dx}\right|\right\}\right)^2\right)^2 +$$
$$\left. + + \left(1 + \left(\sup\left\{\left|\frac{dy(x)}{dx}\right|\right\}\right)^2\right)^2 \right| =$$
$$= \left|\frac{dy_2(x)}{dx} - \frac{dy_1(x)}{dx}\right| \left(6\left(\sup\left\{\left|\frac{dy(x)}{dx}\right|\right\}\right) + \right.$$
$$\left. + 6\left(\sup\left\{\left|\frac{dy(x)}{dx}\right|\right\}\right)^5 + 12\left(\sup\left\{\left|\frac{dy(x)}{dx}\right|\right\}\right)^3\right) \le$$
$$\le 24\left(\sup\left\{\left|\frac{dy(x)}{dx}\right|\right\}\right)^5 \left|\frac{dy_2(x)}{dx} - \frac{dy_1(x)}{dx}\right|. \quad (82)$$

Step 2. We prove that:

$$\left| \left(1 + \left(\frac{dy_2(x)}{dx}\right)^2\right)^3 (\alpha - y_2(x))^2 - \right.$$
$$\left. - \left(1 + \left(\frac{dy_1(x)}{dx}\right)^2\right)^3 (\alpha - y_1(x))^2 \right| \le$$
$$\le 216\left(\sup\left\{\left|\frac{dy(x)}{dx}\right|\right\}\right)^5 \left|\frac{dy_2(x)}{dx} - \frac{dy_1(x)}{dx}\right| +$$
$$24\left(1 + \left(\sup\left\{\left|\frac{dy(x)}{dx}\right|\right\}\right)^6\right) \left|y_2(x) - y_1(x)\right|. \quad (83)$$

In fact, $\forall\, y_1(x), y_2(x) \in P$, since $\alpha < 1$ because $0 < u < 1 - d^*$, it follows that:

$$\left| \left(1 + \left(\frac{dy_2(x)}{dx}\right)^2\right)^3 (1 - d^* - y_2(x))^2 - \right.$$
$$\left. - \left(1 + \left(\frac{dy_1(x)}{dx}\right)^2\right)^3 (1 - d^* - y_1(x))^2 \right| =$$
$$= \left| \left(1 + \left(\frac{dy_2(x)}{dx}\right)^2\right)^3 \left(1 + d^* + y_2^2(x) - 2d^* - \right. \right.$$
$$\left. - 2y_2(x) + 2y_2(x)d^*\right) - \left(1 + \left(\frac{dy_1(x)}{dx}\right)^2\right)^3$$
$$\left. \left(1 + d^* + y_1^2(x) - 2d^* - 2y_1(x) + 2y_1(x)d^*\right) \right| =$$
$$= \left| \left(1 + \left(\frac{y_2(x)}{dx}\right)^2\right)^3 + d^*\left(1 + \left(\frac{dy_2(x)}{dx}\right)^2\right)^3 + \right.$$
$$+ y_2^2(x)\left(1 + \left(\frac{dy_2(x)}{dx}\right)^2\right)^3 -$$
$$- 2d^*\left(1 + \left(\frac{y_2(x)}{dx}\right)^2\right)^3 -$$
$$- 2y_2(x)\left(1 + \left(\frac{dy_2(x)}{dx}\right)^2\right)^3 +$$
$$+ 2y_2(x)d^*\left(1 + \left(\frac{dy_2(x)}{dx}\right)^2\right)^3 -$$
$$- \left(1 + \left(\frac{dy_1(x)}{dx}\right)^2\right)^3 - d^*\left(1 + \left(\frac{dy_1(x)}{dx}\right)^2\right)^3 -$$
$$- y_1^2(x)\left(1 + \left(\frac{dy_1(x)}{dx}\right)^2\right)^3 +$$
$$+ 2d^*\left(1 + \left(\frac{dy_1(x)}{dx}\right)^2\right)^3 +$$
$$+ 2y_1(x)\left(1 + \left(\frac{dy_1(x)}{dx}\right)^2\right)^3 -$$
$$\left. - 2y_1(x)d^*\left(1 + \left(\frac{dy_1(x)}{dx}\right)^2\right)^3 \right| \le$$

$$\le \left| \left(1 + \left(\frac{dy_2(x)}{dx}\right)^2\right)^3 - \left(1 + \left(\frac{dy_1(x)}{dx}\right)^2\right)^3 \right| +$$
$$+ \left| y_2^2(x)\left(1 + \left(\frac{dy_2(x)}{dx}\right)^2\right)^3 - \right.$$
$$- y_2^2(x)\left(1 + \left(\frac{dy_1(x)}{dx}\right)^2\right)^3 +$$
$$+ y_2^2(x)\left(1 + \left(\frac{dy_1(x)}{dx}\right)^2\right)^3 -$$
$$\left. - y_1^2(x)\left(1 + \left(\frac{dy_1(x)}{dx}\right)^2\right)^3 \right| +$$
$$+ d^*\left| \left(1 + \left(\frac{dy_2(x)}{dx}\right)^2\right)^3 - \left(1 + \left(\frac{dy_1(x)}{dx}\right)^2\right)^3 \right| +$$
$$+ 2d^*\left| \left(1 + \left(\frac{dy_2(x)}{dx}\right)^2\right)^3 - \left(1 + \left(\frac{dy_1(x)}{dx}\right)^2\right)^3 \right| +$$
$$+ 2\left| y_2\left(1 + \left(\frac{dy_2(x)}{dx}\right)^2\right)^3 - \right.$$
$$- y_2(x)\left(1 + \left(\frac{dy_1(x)}{dx}\right)^2\right)^3 +$$
$$+ y_2(x)\left(1 + \left(\frac{y_1(x)}{dx}\right)^2\right)^3 -$$
$$\left. - y_1(x)\left(1 + \left(\frac{dy_1(x)}{dx}\right)^2\right)^3 \right| +$$
$$+ 2d^*\left| y_2(x)\left(1 + \left(\frac{dy_2(x)}{dx}\right)^2\right)^3 - \right.$$
$$- y_2(x)\left(1 + \left(\frac{dy_1(x)}{dx}\right)^2\right)^3 +$$
$$+ y_2(x)\left(1 + \left(\frac{dy_1(x)}{dx}\right)^2\right)^3 -$$
$$\left. - y_1(x)\left(1 + \left(\frac{dy_1(x)}{dx}\right)^2\right)^3 \right| \le$$
$$\le 216\left(\sup\left\{\left|\frac{dy(x)}{dx}\right|\right\}\right)^5 \left|\frac{dy_2(x)}{dx} - \frac{dy_1(x)}{dx}\right| +$$
$$+ 24\left(1 + \left(\sup\left\{\left|\frac{dy(x)}{dx}\right|\right\}\right)^6\right) \left|y_2(x) - y_1(x)\right|. \quad (84)$$

Step 3. This point is demonstrated by contradiction. We assume that $y_1(x), y_2(x) \in P$ are two different solutions. By differentiation and exploiting a suitable Green's function $\Sigma(x, s)$, (2) can be written into an equivalent integral formulation. Then, for $i = 1, 2$, we can write:

$$y_i(x) = \int_{-L_1}^{L_1} \Sigma(x, s) \frac{\left(1 + \left(\frac{dy_i(s)}{ds}\right)^2\right)^3}{\theta\mu^2(s, y_i(s), \lambda)} ds =$$
$$= \int_{-L_1}^{L_1} \frac{1}{\theta\lambda^2} \Sigma(x, s)$$
$$\left(1 + \left(\frac{dy_i(s)}{ds}\right)^2\right)^3 (\alpha - y_i(s))^2 ds \quad (85)$$

$$\frac{dy_i(x)}{dx} = \int_{-L_1}^{L_1} \frac{d\Sigma(x, s)}{dx} \frac{\left(1 + \left(\frac{dy_1(s)}{ds}\right)^2\right)^3}{\theta\mu^2(s, y_i(s), \lambda)} ds =$$

$$= \int_{-L_1}^{L_1} \frac{1}{\theta \lambda^2} \frac{d\Sigma(x,s)}{ds}$$

$$\left(1 + \left(\frac{dy_i(s)}{ds}\right)^2\right)^3 (\alpha - y_i(s))^2 ds. \quad (86)$$

Then, it follows that:

$$\|y_1(x) - y_2(x)\|_{C^1([-L_1,L_1])} =$$
$$= \sup_{x \in [-L_1,L_1]} |y_1(x) - y_2(x)| +$$
$$+ \sup_{x \in [-L_1,L_1]} \left|\frac{dy_1(x)}{dx} - \frac{dy_2(x)}{dx}\right|. \quad (87)$$

Then, it follows that:

$$\|T(y_1) - T(y_2)\| =$$
$$= \frac{1}{\theta \lambda^2} \sup_{x \in [-L_1,L_1]} \left| \int_{-L_1}^{L_1} \Sigma(x,s)((1+(y_1'(s))^2)^3) \right.$$
$$(\alpha - y_1(s))^2 ds - \int_{-L_1}^{L_1} \Sigma(x,s)$$
$$\left. ((1+(y_2'(s))^2)^3)(\alpha - y_2(s))^2 ds \right| +$$
$$+ \frac{1}{\theta \lambda^2} \sup_{x \in [-L_1,L_1]} \left| \int_{-L_1}^{L_1} \frac{d\Sigma(x,s)}{dx} \right.$$
$$((1+(y_1'(s))^2)^3)(\alpha - y_1(s))^2 ds -$$
$$- \int_{-L_1}^{L_1} \frac{d\Sigma(x,s)}{dx}((1+(y_2'(s))^2)^3)$$
$$\left. (\alpha - y_2(s))^2 ds \right| \le \frac{1}{\theta \lambda^2} \frac{L_1}{2}$$
$$\sup_{x \in [-L_1,L_1]} \left| \int_{-L_1}^{L_1} [(-(1+(y_1'(s))^2)^3)(\alpha - y_1(s))^2 + \right.$$
$$\left. + (1+(y_2'(s))^2)^3)(\alpha - y_2(s))^2] ds \right| +$$
$$+ \frac{1}{2\theta \lambda^2} \sup_{x \in [-L_1,L_1]} \left| \int_{-L_1}^{L_1} [(-(1+(y_1'(s))^2)^3) \right.$$
$$(\alpha - y_1(s))^2 +$$
$$\left. + (1+(y_2'(s))^2)^3)(\alpha - y_2(s))] ds \right| =$$
$$= \frac{1}{\theta \lambda^2} \left(0.5 + 0.5 L_1\right)$$
$$\sup_{x \in [-L_1,L_1]} \left| \int_{-L_1}^{L_1} [(-(1+(y_1'(s))^2)^3) \right.$$
$$\left. (\alpha - y_1(s))^2 + (1+(y_2'(s))^2)^3)(\alpha - y_2(s))] ds \right|. \quad (88)$$

Considering (84), we can write:

$$\|T(y_1) - T(y_2)\|_{C^1([-L_1,L_1])} \le$$
$$\le \frac{1}{\theta \lambda^2}(0.5 + 0.5 L_1)$$
$$\sup_{x \in [-L_1,L_1]} \left| \int_{-L_1}^{L_1} \left(216\left(\sup\left\{\left|\frac{dy(x)}{dx}\right|\right\}\right)^5 \right.$$

$$\left|\frac{dy_2(s)}{ds} - \frac{dy_1(s)}{ds}\right| +$$
$$+ 24\left(1 + \left(\sup\left\{\left|\frac{dy(x)}{dx}\right|\right\}\right)^6\right)$$
$$|y_2 - y_1|)ds \Bigg| =$$
$$= \frac{1}{\theta \lambda^2}\left(0.5 + 0.5 L_1\right)$$
$$\left(216\left(\sup\left\{\left|\frac{dy(x)}{dx}\right|\right\}\right)^5 2 L_1\right)$$
$$\sup_{s \in [-L_1,L_1]} \left|\frac{dv_2(s)}{ds} - \frac{dv_1(s)}{ds}\right| +$$
$$+ \frac{1}{\theta \lambda^2}\left(0.5 + 0.5 L_1\right)$$
$$\left(24\left(1 + \left(\sup\left\{\left|\frac{dy(x)}{dx}\right|\right\}\right)^6\right) 2 L_1\right)$$
$$\sup_{s \in [-L_1,L_1]} |y_2(s) - y_1(s)|. \quad (89)$$

We observe that, $y_1 = T(y_1)$ and $y_2 = T(y_2)$ so that, exploiting both (87) and (89), we would obtain a contradiction if we write:

$$\begin{cases} 216 \cdot 2 L_1 (\theta \lambda^2)^{-1}\left(0.5 + 0.5 L_1\right) \cdot \\ \cdot \left(\sup\left\{\left|\frac{dy(x)}{dx}\right|\right\}\right)^5 < 1; \\ 24 \cdot 2 L_1 (\theta \lambda^2)^{-1}\left(0.5 + 0.5 L_1\right) \cdot \\ \cdot \left(1 + \left(\sup\left\{\left|\frac{dy(x)}{dx}\right|\right\}\right)^6\right) < 1, \end{cases} \quad (90)$$

that is:

$$\begin{cases} 216\left(\sup\left\{\left|\frac{dy(x)}{dx}\right|\right\}\right)^5 < (L_1(L_1+1))^{-1}\theta\lambda^2 \\ 24\left(1 + \left(\sup\left\{\left|\frac{dy(x)}{dx}\right|\right\}\right)^6\right) < \\ < (L_1(L_1+1))^{-1}\theta\lambda^2. \end{cases} \quad (91)$$

From the first inequality of (91), it makes sense to write:

$$1 + \left(\sup\left\{\left|\frac{dy(x)}{dx}\right|\right\}\right)^6 <$$
$$< 1 + (216 L_1(L_1+1))^{-1}\theta\lambda^2\left(\sup\left\{\left|\frac{dy(x)}{dx}\right|\right\}\right), \quad (92)$$

so (91) assumes the following form:

$$\begin{cases} 1 + \left(\sup\left\{\left|\frac{dy(x)}{dx}\right|\right\}\right)^6 < \\ < 1 + (216 L_1(L_1+1))^{-1}\theta\lambda^2\left(\sup\left\{\left|\frac{dy(x)}{dx}\right|\right\}\right) \\ 1 + \left(\sup\left\{\left|\frac{dy(x)}{dx}\right|\right\}\right)^6 < \\ < (216 L_1(L_1+1))^{-1}\theta\lambda^2. \end{cases} \quad (93)$$

Furthermore, we observe that:

$$(24 L_1(L_1+1))^{-1}\theta\lambda^2 <$$
$$< 1 + (216 L_1(L_1+1))^{-1}\theta\lambda\left(\sup\left\{\left|\frac{dy(x)}{dx}\right|\right\}\right), \quad (94)$$

in fact, starting from (94), it follows that:

$$\left( \sup\left\{ \left| \frac{dy(x)}{dx} \right| \right\} \right) > 9(1 - 24(\theta\lambda^2)^{-1}L_1(L_1+1)). \quad (95)$$

That is definitely true. In fact, supposing, by contradiction, that

$$24L_1(L_1+1)^{-1}\theta\lambda^2 >$$
$$> 1 + (216L_1(L_1+1))^{-1}\theta\lambda^2\left( \sup\left\{ \left| \frac{dy(x)}{dx} \right| \right\} \right), \quad (96)$$

we can write:

$$\left( \sup\left\{ \left| \frac{dy(x)}{dx} \right| \right\} \right) < 9 - 216(\theta\lambda^2)^{-1}L_1(L_1+1) < 0. \quad (97)$$

In other words, $\left( \sup\left\{ \left| \frac{dy(x)}{dx} \right| \right\} \right)$ assumes a negative value (value physically impossible). Then, (63) holds so that the uniqueness of the solution depends on the physical parameters of the membrane. Moreover, $\overline{\lambda}^2$ does not appear, confirming the experimental fact that when $V$ is applied, the membrane moves if $V$ overcomes the inertia $\overline{\lambda}^2$.

## REFERENCES

[1] S. Saponara, A. De Gloria, edts., *Applications in Electronics Pervading Industry, Environment and Society: APPLEPIES 2018*, (Lecture Notes in Electrical Engineering Book 573), Springer, 2019

[2] J. Zhu, "Development Trends and Perspectives of Future Sensors and MEMS/NEMS," *Micromachines*, vol. 11, no. 7, 2020

[3] J.A. Pelesko, D. H. Bernstein, *Modeling MEMS and NEMS*, CRC Press Company, Boca Raton London New York Washington D.C., 2003.

[4] D. Ortloff, et al., *MEMS Product Engineering*, Springer-Verlag Wien, 2014.

[5] M. Gad-el-Hak edt., *The MEMS Handbook*, CRC Press, 2015.

[6] F. Khoshnoud, and C. W. de Silva, "Recent advances in MEMS sensor technology–biomedical applications," *IEEE Instrumentation Measurement Magazine*, vol. 15., no. 1, pp. 8-14, 2012.

[7] C. Walk, M. Wiemann, M. Goertz, Weidenmueller, A. Jupe, K. Seidl, "A Piezoelectric Flexural Plate Wave (FPW) Bio-MEMS Sensor with Improved Molecular Mass Detection for Point-of-Care Diagnostics," *Current Directions in Biomedical Engineering*, vol. 5, no. 1, pp. 265-268, 2019.

[8] C. M. Puleo, H. C. Yeh, T.H. Wang, "Applications of MEMS Technologies in Tissue Engineering," *Tissue Engineering*, vol. 13, no. 12, pp. 2839-2854, 2007.

[9] P. A. Kumar, K. Srinivasa Rao, and K. Girija Sravani, "Design and simulation of millimeter wave reconfigurable antenna using iterative meandered RF MEMS switch for 5G mobile communications," *Microsystem Technologies*, pp. 1-11, 2019.

[10] A. A. Zhilenkov, and D. Denk, "Based on MEMS sensors man-machine interface for mechatronic objects control," *IEEE Conference EIConRus*, pp. 1100-1103, 2017.

[11] A. K. Mohammadi, and N. A. Ali, "Effect of high electrostatic actuation on thermoelastic damping in thin rectangular microplate resonators," *Journal of Theoretical and Applied Mechanics*, vol. 53, no. 2, pp. 317-319, 2015.

[12] F. Wang, L. Zhang, L. Li, Z. Qiao, and Q. Cao, "Design and Analysis of the Elastic-Beam Delaying Mechanism in a Micro-Electro-Mechanical Systems Device," *Micromachines*, vol. 9, no. 11, pp. 567, 2018.

[13] A. L. Herrera-May, L. A. Aguilera-Cortés, P. J. García-Ramírez, and E. Manjarrez, "Resonant magnetic field sensors based on MEMS technology," *Sensors*, vol. 9, no. 10, pp. 7785-7813, 2009.

[14] P. Esposito, N. Ghoussoub, Y. Guo, *Mathematical analysis of partial differential equations modeling electrostatic MEMS*, American Mathematical Soc., 2010.

[15] H. Javaheri, P. Ghanati, and S. Azizi, "A Case Study on the Numerical Solution and Reduced Order Model of MEMS," *Sensing and Imaging*, vol. 19, no. 1, pp.3, 2018.

[16] M. Mashinchi Joubari, R. Asghari, "Analytical Solution for Nonlinear Vibration of Micro-Electromechanical System (MEMS) by Frequency-Amplitude Formulation Method," *The Journal of Mathematics and Computer Science*, vol. 4, no. 3, pp. 371-379, 2012.

[17] D. Cassani, and N. Ghoussoub, "On a fourth order elliptic problem with a singular nonlinearity," *Advanced Nonlinear Studies*, vol. 9, no. 1, pp. 177-197, 2009.

[18] D. Cassani, L. Fattorusso, A. Tarsia, "Nonlocal dynamic problems with singular nonlinearities and applications to MEMS," in *Analysis and topology in nonlinear differential equations*, pp. 187-206, Birkhäuser, Cham, 2014

[19] P. Di Barba, L. Fattorusso, M. Versaci, "Electrostatic field in terms of geometric curvature in membrane MEMS devices," *Communications in Applied and Industrial Mathematics*, vol. 8, no. 1, pp.165-184, 2017.

[20] G. Angiulli, J. Jannelli, F. C. Morabito, M. Versaci, "Reconstructing the Membrane Detection of a $1D$ Electrostatic-Driven MEMS Device by the Shooting Method: Convergence Analysis and Ghost Solutions Identification," *Comp. Appl. Math*, vol. 37, pp. 4484-4498, 2018, doi.org/10.1007/s40314-017-0564-4.

[21] A. Iserles, *A First Course in the Numerical Analysis of Differential Equations*, Cambridge University Press, 2009.

[22] A. Quarteroni, R. Sacco, F. Saleri, *Numerical MAthematics*, Springer-Verlag Berlin Heidelberg, 2007.

[23] M. Versaci, G. Angiulli, L. Fattorusso, A. Jannelli, "On the uniqueness of the solution for a semi-linear

elliptic boundary value problem of the membrane MEMS device for reconstructing the membrane profile in absence of ghost solutions," *International Journal of Non-Linear Mechanics*, vol. 109, pp. 24-31, 2019.

[24] M.P. do Carmo, *Differential Geometry of Curves and Surfaces*, Prentice-Hall, Inc., Englewood Cliffs, New Jersey, 2000.

[25] C. Lopez, *MATLAB Differential Equations*, APress, Springer, 2014.

[26] M. Versaci, G. Angiulli, A. Jannelli, "Recovering of the Membrane Profile of an Electrostatic Circular MEMS by a Three-Stage Lobatto Procedure: a Convergence Analysis in Absence of Ghost Solutions," Mathematics vol. 19, no. 2, pp. 360, 2020, https://doi.org/10.3390/s19020360

[27] A. Jannelli, "Numerical Solutions of Fractional Differential Equations Arising in Engineering Sciences," *Mathematics*, vol. 8, pp.215, 2020, doi: 10.3390/math8020215.

[28] P. Ghosh, Numerical, Symbolic and Statistical Computing for Chemical Engineers Using MatLab®, Delhi 110092, PHI, 2018.

ALESSANDRA JANNELLI received her Ph.D. degre in Mathematics from the University of Messina, Italy, in 2000. Since 2009, she serves as an Assistant Professor of Numerical Analysis at the Department of Mathematical and Computer Science, Physical Science and Hearth Sciences, at the same university. Her research activity is mainly focused on mathematical models and numerical methods for problems related to non-destructive industrial controls, transport-reaction-diffusion problems, free frontier formulations defined on infinite domains, and for fractional derivative problems. She is a member of the Italian Society for Industrial and Applied Mathematics (SIMAI), and an aggregate member of the Accademia Peloritana dei Pericolanti.

GIOVANNI ANGIULLI (SM, 15) received his Ph.D. degree in Electronic Engineering and Computer Science from the University of Naples Federico II, in 1998. Since 1999, he has been with the Department of Information, Infrastructures, and Sustainable Energy (DIIES, formerly DIMET) at University Mediterranea of Reggio Calabria, Italy, as an Adjunct Professor. His main research activities concern Computational Electromagnetics, Group Theory methods, and Surrogate Modelling Techniques applied to model microwave circuits and antennas. In the last years, he worked also on microwave imaging to detect female breast tumors and Ground Penetrating Radar applications in cultural heritage. He is a Senior Member of IEEE, and a Member of the Institute of Electronics, Information and Communication Engineers (IEICE). He serves as an Associate Editor for IEEE Access. In recognition of his exceptional contributions, he has been honored as an Outstanding Associate Editor for the year 2018 by the IEEE Access Editorial Board.

• • •

MARIO VERSACI (M'16, SM'17) received his degree in civil engineering in 1994 from the "Mediterranea" University, Italy, where he also he received, in 1999, a Ph.D. in electronic engineering. He also received the Diplome d'Etudes Approfondites (Genie Electrique) at the Grenoble Electrotechnics Lab. In the "Mediterranea" university, he serves as both Associate Professor of electrical engineering and scientific head of the NDT/NDE Lab. In 2018 he also received a degree in mathematics from the University of Messina. His research focus on soft computing techniques for NDT/NDE, image processing and MEMS/NEMS. He has authored more than 110 papers published in international journalls/conference proceedings in several fields of engineering and mathematics. He also served as Member of the Accademia Peloritana dei Pericolanti.